HNPS Advances in Nuclear Physics

Vol 14 (2005)

HNPS2005

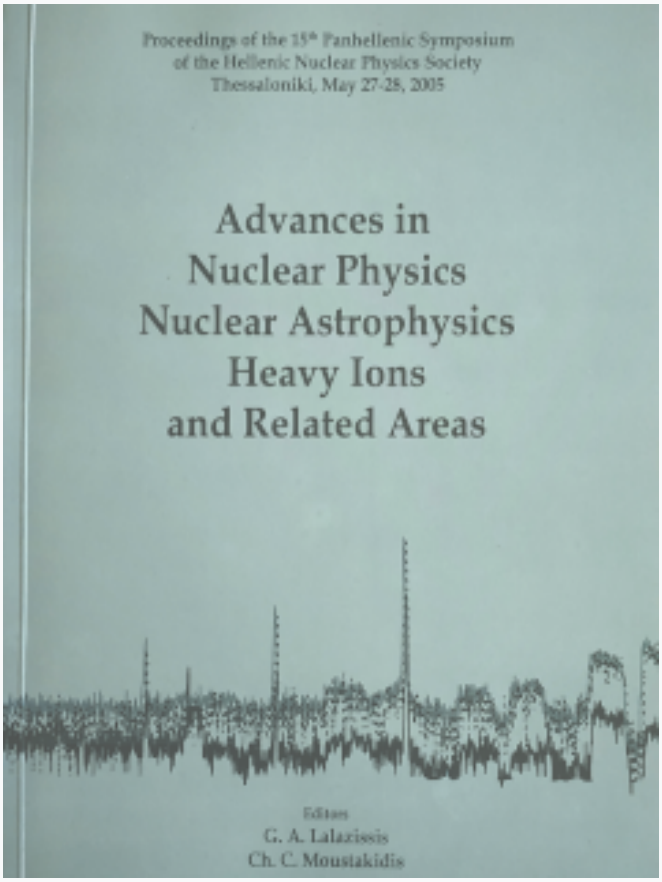

Analytic description of critical point actinides in a transition from octupole deformation to octupole vibrations

Dennis Bonatsos, D. Lenis, N. Minkov, D. Petrellis, P. Yotov

doi: 10.12681/hnps.2245

Analytic description of critical point actinides in a transition from octupole deformation to octupole vibrations

Dennis Bonatsos [a], D. Lenis [a], N. Minkov [b], D. Petrellis [a], P. Yotov [b]

[a] *Institute of Nuclear Physics, N.C.S.R. "Demokritos", GR-15310 Aghia Paraskevi, Attiki, Greece*

[b] *Institute for Nuclear Research and Nuclear Energy, Bulgarian Academy of Sciences, 72 Tzarigrad Road, BG-1784 Sofia, Bulgaria*

Abstract

An analytic collective model in which the relative presence of the quadrupole and octupole deformations is determined by a parameter (ϕ_0), while axial symmetry is obeyed, is developed. The model [to be called the analytic quadrupole octupole axially symmetric model (AQOA)] involves an infinite well potential, provides predictions for energy and $B(EL)$ ratios which depend only on ϕ_0, draws the border between the regions of octupole deformation and octupole vibrations in an essentially parameter-independent way, and describes well ^{226}Th and ^{226}Ra, for which experimental energy data are shown to suggest that they lie close to this border. The similarity of the AQOA results with $\phi_0 = 45^\circ$ for ground state band spectra and $B(E2)$ transition rates to the predictions of the X(5) model is pointed out.

1 Introduction

The critical point symmetries E(5) [1] and X(5) [2] developed up to now treat the quadrupole degree of freedom alone. In the present work an Analytic Quadrupole Octupole Axially symmetric (AQOA) model is developed, aiming at the description of the transition from octupole deformation [3] to octupole vibrations in the light actinides.

In Section 2 the AQOA model is formulated, while numerical results are compared to experiment in Section 3, and Section 4 contains discussion of the present results and plans for further work.

2 The AQOA model

We consider a nucleus in which quadrupole deformation (β_2) and octupole deformation (β_3) coexist. We take only axially symmetric deformations into account, which implies that the γ degrees of freedom are ignored, as in the Davydov–Chaban approach [4]. The body-fixed axes x', y', z' are taken along the principal axes of inertia of the (axially symmetric) nucleus, while their orientation relative to the laboratory-fixed axes x, y, z is described by the Euler angles $\theta = \{\theta_1, \theta_2, \theta_3\}$. The Hamiltonian reads [5,6]

$$H = -\sum_{\lambda=2,3} \frac{\hbar^2}{2B_\lambda} \frac{1}{\beta_\lambda^3} \frac{\partial}{\partial \beta_\lambda} \beta_\lambda^3 \frac{\partial}{\partial \beta_\lambda} + \frac{\hbar^2 \hat{L}^2}{6(B_2\beta_2^2 + 2B_3\beta_3^2)} + V(\beta_2, \beta_3) \qquad (1)$$

where B_2, B_3 are the mass parameters.

We seek solutions of the Schrödinger equation of the form [5]

$$\Phi_L^{\pm}(\beta_2, \beta_3, \theta) = (\beta_2\beta_3)^{-3/2} \Psi_L^{\pm}(\beta_2, \beta_3) |LM0, \pm\rangle, \qquad (2)$$

where the function $|LM0, \pm\rangle$ describes the rotation of an axially symmetric nucleus with angular momentum projection M onto the laboratory-fixed z-axis and projection $K = 0$ onto the body-fixed z'-axis. The moment of inertia with respect to the symmetry axis z' is zero, implying that levels with $K \neq 0$ lie infinitely high in energy [5]. Therefore in this model we are restricted to states with $K = 0$ only. The function $|LM0, +\rangle$ transforms according to the irreducible representation (irrep) A of the group D_2, while the function $|LM0, -\rangle$ transforms according to the irrep B_1 of the same group [5,6]. The general form of these functions is [7]

$$|LMK, \pm\rangle = \sqrt{\frac{2L+1}{16\pi^2(1+\delta_{K0})}} (D^L_{K,M}(\theta) \pm (-1)^L D^L_{-K,M}(\theta)). \qquad (3)$$

In the special case of $K = 0$ it is clear that $|LM0, +\rangle \neq 0$ for $L = 0$, 2, 4, ..., while $|LM0, -\rangle \neq 0$ for $L = 1$, 3, 5, ... The functions $\Psi_L^+(\beta_2, \beta_3)$ and $\Psi_L^-(\beta_2, \beta_3)$ are respectively symmetric and antisymmetric with respect to reflection in the plane $x'y'$, and therefore describe states with positive and negative parity respectively [6].

Using the solutions of Eq. (2) for the Hamiltonian of Eq. (1), introducing [5,6] $\tilde{\beta}_2 = \beta_2\sqrt{B_2/B}$, $\tilde{\beta}_3 = \beta_3\sqrt{B_3/B}$, $B = B_2 + B_3/2$, reduced energies $\epsilon = (2B/\hbar^2)E$ and reduced potentials $u = (2B/\hbar^2)V$ [1,2], polar coordinates (with $0 \leq \tilde{\beta} < \infty$ and $-\pi/2 \leq \phi \leq \pi/2$) [5,6] $\tilde{\beta}_2 = \tilde{\beta}\cos\phi$, $\tilde{\beta}_3 = \tilde{\beta}\sin\phi$, $\tilde{\beta} =$

$\sqrt{\tilde{\beta}_2^2 + \tilde{\beta}_3^2}$, and assuming the potential to be of the form $u(\tilde{\beta}, \phi) = u(\tilde{\beta}) + u(\tilde{\phi}^{\pm})$, where $u(\tilde{\phi}^{\pm})$ is supposed to be of the form of two very steep harmonic oscillators centered at the values $\pm\phi_0$, i.e.

$$u(\tilde{\phi}^{\pm}) = \frac{1}{2}c(\phi \mp \phi_0)^2 = \frac{1}{2}c(\tilde{\phi}^{\pm})^2, \qquad \tilde{\phi}^{\pm} = \phi \mp \phi_0, \tag{4}$$

with c being a large constant, the Schrödinger equation corresponding to the Hamiltonian of Eq. (1) is separated into

$$\left[-\frac{\partial^2}{\partial\tilde{\beta}^2} - \frac{1}{\tilde{\beta}}\frac{\partial}{\partial\tilde{\beta}} + \frac{1}{\tilde{\beta}^2}\left(\frac{L(L+1)}{3(1+\sin^2\phi_0)} + \frac{3}{\sin^2 2\phi_0}\right) + u(\tilde{\beta}) - \epsilon_{\tilde{\beta}}(L)\right]\psi_L^{\pm}(\tilde{\beta}) = 0, \tag{5}$$

and

$$\left[-\frac{1}{\langle\tilde{\beta}^2\rangle}\frac{\partial^2}{\partial(\tilde{\phi}^{\pm})^2} + u(\tilde{\phi}^{\pm}) - \epsilon_{\phi}\right]\chi(\tilde{\phi}^{\pm}) = 0, \tag{6}$$

where $\Psi_L^{\pm}(\tilde{\beta}, \phi) = \psi_L^{\pm}(\tilde{\beta})(\chi(\tilde{\phi}^{+}) \pm \chi(\tilde{\phi}^{-}))/\sqrt{2}$, while $\langle\tilde{\beta}^2\rangle$ is the average of $\tilde{\beta}^2$ over $\psi^{\pm}(\tilde{\beta})$, and $\epsilon_L = \epsilon_{\tilde{\beta}}(L) + \epsilon_{\phi}$. Eq. (6) for the potential of Eq. (4) becomes a simple harmonic oscillator equation (n_{ϕ} being the relevant quantum number), while in the case in which $u(\tilde{\beta})$ is an infinite well potential ($u(\tilde{\beta}) = 0$ if $\tilde{\beta} \leq \tilde{\beta}_W$; $u(\tilde{\beta}) = \infty$ if $\tilde{\beta} > \tilde{\beta}_W$), using the definitions $\epsilon_{\tilde{\beta}} = k_{\tilde{\beta}}^2$, $z = \tilde{\beta}k_{\tilde{\beta}}$, Eq. (5) is brought into the form of a Bessel equation

$$\frac{d^2\psi_\nu^{\pm}}{dz^2} + \frac{1}{z}\frac{d\psi_\nu^{\pm}}{dz} + \left[1 - \frac{\nu^2}{z^2}\right]\psi_\nu^{\pm} = 0, \quad \nu = \sqrt{\frac{L(L+1)}{3(1+\sin^2\phi_0)} + \frac{3}{\sin^2 2\phi_0}}. \tag{7}$$

Then the boundary condition $\psi_\nu^{\pm}(\tilde{\beta}_W) = 0$ determines the spectrum

$$\epsilon_{\tilde{\beta},s,\nu} = \epsilon_{\tilde{\beta},s,\phi_0,L} = (k_{s,\nu})^2, \qquad k_{s,\nu} = x_{s,\nu}/\tilde{\beta}_W, \tag{8}$$

and the eigenfunctions

$$\psi_{s,\nu}^{\pm}(\tilde{\beta}) = \psi_{s,\phi_0,L}^{\pm}(\tilde{\beta}) = c_{s,\nu}J_\nu(k_{s,\nu}\tilde{\beta}), \tag{9}$$

where $x_{s,\nu}$ is the sth zero of the Bessel function $J_\nu(z)$, while $c_{s,\nu}$ are normalization constants, determined from the condition $\int_0^{\tilde{\beta}_W} |\psi_{s,\nu}^{\pm}(\tilde{\beta})|^2\tilde{\beta}d\tilde{\beta} = 1$ to be $c_{s,\nu} = \sqrt{2}/J_{\nu+1}(k_{s,\nu})$. The notation has been kept similar to Ref. [2].

The total energy in the present model is then

$$E(s, L, \phi_0, n_\phi) = E_0 + A\epsilon_{\tilde{\beta},s,\phi_0,L} + Bn_\phi. \tag{10}$$

In the axial case used here the electric multipole operators are [5]

$$T^{(E1)}_\mu = t_1\beta_2\beta_3 D^{(1)}_{\mu,0}(\theta), \quad T^{(E2)}_\mu = t_2\beta_2 D^{(2)}_{\mu,0}(\theta), \quad T^{(E3)}_\mu = t_3\beta_3 D^{(3)}_{\mu,0}(\theta). \tag{11}$$

$B(EL)$s are calculated using the standard techniques, the final result being

$$B(EL; L_i \to L_f) = c(c_{s_i,\nu_i}c_{s_f,\nu_f})^2(L_iLL_f|000)^2(I^{(EL)}_{\tilde{\beta}})^2, \tag{12}$$

where L = 1-3, the integrals are $I^{(E2)}_{\tilde{\beta}} = I^{(E3)}_{\tilde{\beta}} = \int \tilde{\beta}^2 J_{\nu_i}(k_{s_i,\nu_i}\tilde{\beta})J_{\nu_f}(k_{s_f,\nu_f}\tilde{\beta})d\tilde{\beta}$, while in $I^{(E1)}_{\tilde{\beta}}$ an extra factor of $\tilde{\beta}$ appears, and all constants have been absorbed in c.

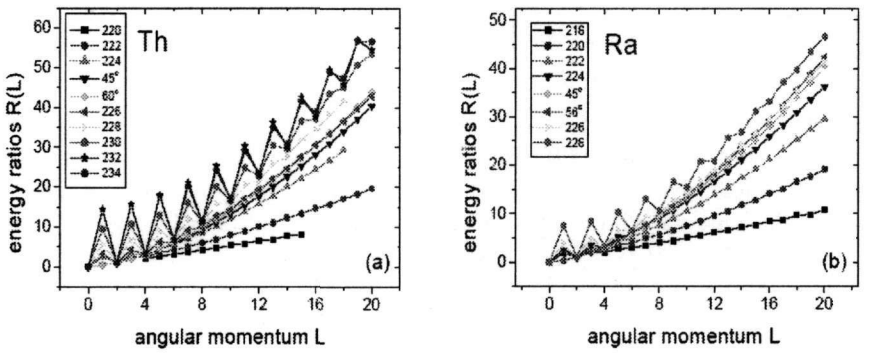

Fig. 1. (a) Experimental energy ratios $R(L) = E(L)/E(2^+_1)$ for ^{220}Th [8], ^{222}Th [9], ^{224}Th [10], ^{226}Th [11], ^{228}Th [12], ^{230}Th [13], ^{232}Th [13,14], and ^{234}Th [13], compared to theoretical predictions for $\phi = 45°$ and $\phi = 60°$ (b) Same for ^{218}Ra [15,16], ^{220}Ra [8], ^{222}Ra [13,17], ^{224}Ra [13,17], ^{226}Ra [13,17], and ^{228}Ra [13], compared to theoretical predictions for $\phi = 45°$ and $\phi = 56°$.

3 Numerical results and comparison to experiment

Spectra for the ground state band and the negative parity band associated with it ($s = 1$), as well as for the first excited band ($s = 2$) and the second excited band ($s = 3$), are quite stable in the region $30° \leq \phi_0 \leq 60°$, while at the limiting cases near $\phi_0 = 0°$ and $90°$ the rigid rotor results are obtained, corresponding to a pure rotational spectrum for the ground state band and the associated negative parity band, while the excited bands are pushed to

infinity. $B(EL)$ transition rates also possess a smooth behaviour within the same region.

Comparing AQOA to X(5), it is clear that the ground state band of X(5) lies a little lower and has slightly higher intraband $B(E2)$s than the ground state band of the AQOA model with $\phi_0 = 45^o$, while for the $s = 2$ and $s = 3$ bands the AQOA model predictions for $\phi_0 = 45^o$ are larger than the X(5) values by almost a factor of two. The position of the 0_2^+ state becomes therefore an important factor in the process of comparison to experiment.

Experimental data for the ground state and related negative parity bands of $^{220-234}$Th are shown in Fig. 1(a). It is clear that ^{226}Th lies on the border between two different regions. Below ^{226}Th the odd–even staggering is very small, while from ^{228}Th up the odd–even staggering is becoming much larger, increasing with the neutron number N. It is clear that below ^{226}Th the situation corresponds to octupole deformation, in which the ground state band and the negative parity band merge into a single band, while above ^{226}Th the picture is corresponding to octupole vibrations, i.e. the negative parity band is a rotational band built on an octupole bandhead, thus lying systematically higher than the ground state band. Theoretical predictions for $\phi = 45^o$ lie a little below ^{226}Th, while the $\phi = 60^o$ results follow the ^{226}Th data very closely. A similar picture is observed in $^{218-228}$Ra, shown in Fig. 1(b), where ^{226}Ra appears to be the border nucleus.

As far as the 0_2^+ bandhead is concerned, the experimental values (normalized to the 2_1^+ state) are 12.186 for ^{226}Ra and 11.152 for ^{226}Th, in good agreement with the 11.226 and 12.410 values predicted by the AQOA model for the ϕ_0 values of 56° and 60° used in Fig. 1 . It should be noticed that the normalized 0_2^+ bandhead is lying close to this height for all Ra and Th isotopes for which data exist, namely ^{222}Ra (8.225), ^{224}Ra (10.861), ^{228}Ra (11.300), ^{228}Th (14.402), ^{230}Th (11.934), ^{232}Th (14.794), ^{234}Th (16.347), with data taken from the references used in Fig. 1 .

Considering the AQOA model as an extension of the X(5) framework involving negative parity states implies that the search for X(5)-like nuclei in the light actinides, where the presence of low-lying negative parity bands is important, should be focused on nuclei with $R(4)$ ratio close to 3.0 and 0_2^+ bandhead higher than the X(5) value of 5.65 .

4 Discussion

The analytic quadrupole octupole axially symmetric (AQOA) model introduced in this work describes well the border between octupole deformation

and octupole vibrations in the light actinides, which corresponds to ^{226}Th and ^{226}Ra in the Th and Ra isotopic chains respectively. The inclusion of staggering in the present model, as well as its application to the rare earth region near $A = 150$, where octupole deformation is known to occur [3], are also of interest and will be pursued in Ref. [18].

References

[1] F. Iachello, Phys. Rev. Lett. **85**, 3580 (2000).

[2] F. Iachello, Phys. Rev. Lett. **87**, 052502 (2001).

[3] P. A. Butler and W. Nazarewicz, Rev. Mod. Phys. **68**, 349 (1996).

[4] A. S. Davydov and A. A. Chaban, Nucl. Phys. **20**, 499 (1960).

[5] A. Ya. Dzyublik and V. Yu. Denisov, Yad. Fiz. **56**, 30 (1993) [Phys. At. Nucl. **56**, 303 (1993)].

[6] V. Yu. Denisov and A. Ya. Dzyublik, Nucl. Phys. A **589**, 17 (1995).

[7] A. Bohr and B. R. Mottelson, Nuclear Structure, Vol. II (Benjamin, New York, 1975).

[8] A. Artna-Cohen, Nucl. Data Sheets **80**, 157 (1997).

[9] Y. A. Akovali, Nucl. Data Sheets **77**, 271 (1996).

[10] A. Artna-Cohen, Nucl. Data Sheets **80**, 227 (1997).

[11] Y. A. Akovali, Nucl. Data Sheets **77**, 433 (1996).

[12] A. Artna-Cohen, Nucl. Data Sheets **80**, 723 (1997).

[13] J. F. C. Cocks *et al.*, Nucl. Phys. A **645**, 61 (1999).

[14] M. R. Schmorak, Nucl. Data Sheets **63**, 139 (1991).

[15] Y. A. Akovali, Nucl. Data Sheets **76**, 457 (1995).

[16] N. Schulz *et al.*, Phys. Rev. Lett. **63**, 2645 (1989).

[17] J. F. C. Cocks *et al.*, Phys. Rev. Lett. **78**, 2920 (1997).

[18] D. Bonatsos, D. Lenis, N. Minkov, D. Petrellis, and P. Yotov, these proceedings.